CROATICA CHEMICA ACTA
CCACAA, ISSN 0011-1643, e-ISSN 1334-417X
Croat. Chem. Acta **83** (3) (2010) 275–282.
CCA-3417

Original Scientific Article

Synthesis, Structural Characterization and Magnetic Properties of Iron Boride Nanoparticles with or without Silicon Dioxide Coating

Mislav Mustapić,[a] Damir Pajić,[a] Nikolina Novosel,[a,*] Emil Babić,[a] Krešo Zadro,[a] Marina Cindrić,[b] Joseph Horvat,[c] Željko Skoko,[a] Mirjana Bijelić,[a] and Andrey Shcherbakov[c]

[a]*Department of Physics, Faculty of Science, University of Zagreb, Bijenička cesta 32, HR-10000 Zagreb, Croatia*
[b]*Department of Chemistry, Faculty of Science, University of Zagreb, Horvatovac 102a, HR-10000 Zagreb, Croatia*
[c]*Institute for Superconducting and Electronic Materials, University of Wollongong, Northfields Avenue, NSW 2522 Wollongong, Australia*

RECEIVED JANUARY 19, 2010; REVISED FEBRUARY 26, 2010; ACCEPTED MARCH 3, 2010

Abstract. Nanoparticles of iron boride (Fe_2B, Fe_2B coated in SiO_2, $Fe_xCo_{2-x}B$ coated in SiO_2) were synthesized using the reduction of metal ions by sodium borohydride. X-ray diffraction confirms the amorphicity of the coated compounds and scanning electron microscope imaging revealed the nanoparticulated structure of all compounds. The splitting between zero-field-cooled and field-cooled temperature dependent magnetization curves point to the blocking of superparamagnetic particles magnetization. Magnetic hysteresis loops are however consistent with the combined effects of blocked superparamagnetic and ferromagnetic (multidomain) particles. The observed quite complex magnetic behaviour is in accordance with structural studies, where additional phases and broad distribution of particle sizes were identified.

Keywords: Fe-B, Fe-Co-B, SiO_2 coating, magnetic nanoparticles, amorphous alloy

INTRODUCTION

Magnetic nanoparticles have received a considerable attention as they pose the intriguing questions about the behaviour of matter on such a small scale and because of revealing the processes not observable in the macroscopic world. They are a subject of intense research in many disciplines.

Magnetism in nanoparticles is governed by large proportion of surface to volume in the whole sample. It affects the magnetic ordering, that becomes very complex, including the surface disorder and spin canting in the core.[1] More striking is the possibility to observe the quantum tunneling of magnetization, as an additional process of flipping their magnetic moment besides the classical thermal activation.[2]

Through chemical synthesis it is possible to tune magnetic properties of nanoparticles at least partially. The composition of the particles affects the basic magnetic properties and allows the tuning of interactions that control magnetic ordering. Besides the well defined crystal structure, an amorphous matrix is also possible. Other important issue is the coating of particles. It has a role of stabilizing the composition (for example against oxidation of the core), isolating the particles mutually to decrease their magnetic interaction, and to influence the surface magnetic ordering among particles.

Besides the interesting physical properties, the magnetic nanoparticles find their application in profitable technologies. Magnetic data storage requires an enhancement of thermal stability of the nanoparticle magnetization.[3] Furthermore, all of the above mentioned issues are of importance in biomedicine, where they offer some attractive possibilities.[4] Inner structure of particles plays a role in response to the applied magnetic fields, that could be used for hyperthermia treatment, transport of the particles through tissue guided by an applied field, and enhancement of the magnetic resonance imaging contrasts. Coating of the particles is important through the functionalization of the surface that becomes able to bind the desired substances and release them at desired place.

All of that gives an impulse to study the properties of magnetic nanoparticles synthesized using different methods. For example, the sol-gel auto-ignition method is relatively simple by any means for production of ferrite particles,[5] but does not allow for coating of the particles with desired compounds. Numerous other synthesis techniques give broad variety of core-shell structured particles with more or less narrow

* Author to whom correspondence should be addressed. (E-mail: nnovosel@phy.hr)

particle size distribution, suitable for application in biomedicine.[6]

In this work we present the synthesis route for production of Fe_2B nanoparticles uncoated and coated in SiO_2, as well as coated FeCoB nanoparticles ($Fe_xCo_{2-x}B$). Their structural and magnetic characterization is performed in order to compare their properties. This is of importance for our next goal of implementation of these magnetic particles into superconductors as a method for potential improvement of their electromagnetic properties.[7] Therefore, the role of silica shell, which is important for stabilization and separation of particles, is studied here through magnetic properties.

2 SYNTHESIS AND EXPERIMENTAL PROCEDURES

Amorphous nanoparticles of Fe-B and Fe-Co-B alloys were obtained by reduction of aqueous solutions of metallic salts of $FeSO_4$ and $CoCl_2$ with $NaBH_4$ solution, as reported previously.[8] We performed the experiments with different reactants based on the procedure known to be efficient for amorphous particles production: 0.1 M solution of $FeSO_4$ or $CoCl_2$, 1.0 M solution of $NaBH_4$ or KBH_4, quantity ratio of $FeSO_4$ to $NaBH_4 \geq 0.6$ (we used 1:1) and reaction temperature ≤ 279 K (Ref. 9).

Fe-B particles coated with SiO_2[10] were prepared with 1.0 M $NaBH_4$ solution, which was added rapidly with stirring to the solution of 0.1 M $FeSO_4$. The volume ratio of main reactans was 1:1 (we used 70 ml of each). After adding $NaBH_4$ we added immediately 70 ml ethanol 96% which contained 1.5 ml tetraethoxysilan (TEOS) and 2 ml of 0.4 M NH_4OH. To produce the particles without SiO_2 coating we omitted the ethanol solution of TEOS. To prepare the particles of Fe-Co-B coated with SiO_2 we added the same quantities of 0.1 M solution of $CoCl_2$ and 0.1 M solution of $FeSO_4$ to the 1.0 M solution of $NaBH_4$ so that the quantity ratio of $CoCl_2$ and $FeSO_4$ to $NaBH_4$ is ≥ 0.6.

We performed the syntheses in a closed system with argon atmosphere and the solutions were bubbled with argon one hour prior to the synthesis and one hour after the mixing of solutions. A black powder was collected and washed with distilled water to remove residual ions, then it was rinsed with acetone to remove water and finally dried in vacuum. Several syntheses differing in the duration of reaction, the contents and concentrations of the components and the reaction temperatures were performed.

The obtained samples were examined at room temperature by X-ray powder diffraction (XRD) using an automatic Philips diffractometer, model PW1820 (Cu-K_α radiation, graphite monochromator, proportional counter), in Bragg-Brentano geometry. The diffraction intensites were measured in the angular range $10° \leq 2\theta \leq 70°$. Step size was set to 0.02° 2θ with measuring time of 2 s per step.

Nanostructure was studied using scanning electron microscope (SEM) imaging performed with the microscope JEOL JSM7500FA cold Field Emission Gun Scanning Electron Microscope (FEGSEM).

The powder samples for magnetic measurements were dispersed and fixed in parafin within measuring ampoule to avoid rotation of particles/grains in changing magnetic field. Magnetization measurements were performed using commercial Quantum Design MPMS5 magnetometer equiped with SQUID (Superconducting Quantum Interferometer Device). Magnetic hysteresis loops $M(H)$ were measured in the field range ±5 T at temperatures 5 and 290 K. Temperature dependence of magnetization $M(T)$ for temperature interval 5−300 K in different applied magnetic fields H was measured in two modes: after zero field cooling (ZFC curves) and after field cooling (FC curves), with the same field as used for measurement. Both, ZFC and FC data were measured upon warming the sample. Besides the SQUID magnetometer, we used vibrating sample magnetometer PAR EG&G VSM 4500 for measuremets of magnetic hysteresis loops at room temperature with applied fields up to ± 0.95 T.

3 RESULTS AND DISCUSSION

3.1 Structural characterization

The expected chemical reaction forming the core of the Fe_2B particles is based on reduction of metal ions by sodium borohydride, according to the following chemical equation:

$$4FeSO_4 + 8NaBH_4 + 18H_2O \rightarrow 2Fe_2B + 6B(OH)_3 + 25H_2 + 4Na_2SO_4. \quad (1)$$

In presence of oxygen during the reaction process the oxidation of Fe_2B into elementary α-Fe is possible:

$$4Fe_2B + 3O_2 \rightarrow 8Fe + 2B_2O_3. \quad (2)$$

For production of FeCoB particles we used $CoCl_2$ in addition to $FeSO_4$. The ratio between Fe and Co amount in final product is not strictly 1. Here also the oxidation during process could result with elementary iron or cobalt phases.

Since we did not measure the actual compositions of our particles, we use here the nominal compositions Fe_2B and FeCoB, *i.e.* those consistent with the quantities of reactants. However, the XRD results and also the magnetizations of Fe_2B particles (described below) are quite consistent with the dominant Fe_2B-like phase.

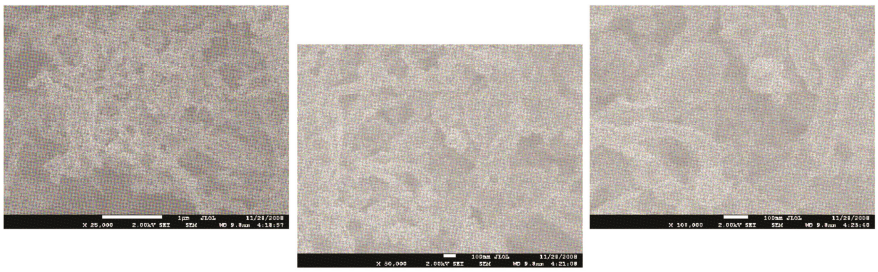

Figure 2. SEM images of Fe_2B particles.

(Also, the composition of our reacently prepared Fe_2B and NiCoB coated and uncoated particles determined by EDS were quite close, to within few percents, to their nominal concentrations.)

Figure 1 shows XRD patterns of our samples. In a pattern of Fe_2B+SiO_2 sample (middle curve, red trace) two broad maxima centered at ≈28° and ≈45° 2θ were observed; their broadness indicated the amorphous state. The position of the broad maximum centered at 45° 2θ otherwise corresponds to the strongest diffraction line 211 of crystalline Fe_2B, whereas broad maximum around 28° probably arises from amorphous silica.[10] Several rather sharp maxima were also detected, belonging to a crystalline SiO_2 (probably cristobalite) phase, present in traces. These maxima are probably associated with precipitated (ellipsoidal) pure SiO_2 particles and not with shells of magnetic particles. Small fraction of precipitated silica was also detected in Ref. 10. However, in our case most of the particles were amorphous (Figure 1), whereas those in Ref. 10 showed fine crystalline domains with crystallite size ≤ 5 nm.

The blue trace in Figure 1 (lower curve) shows XRD pattern of SiO_2 coated $Fe_xCo_{2-x}B$ particles. The alloy was in amorphous state which is clearly indicated by two broad maxima centered at ≈28° and ≈45° 2θ. No crystalline peaks were present in this pattern.

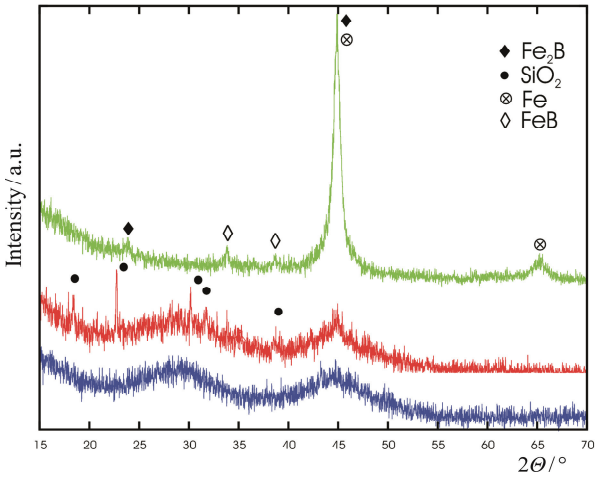

Figure 1. X-ray diffraction patterns of Fe_2B (green, upper), Fe_2B/SiO_2 (red, middle) and $Fe_xCo_{2-x}B/SiO_2$ (blue, bottom) particles.

The upper (green) trace in Figure 1 shows the XRD pattern of Fe_2B sample. This sample was crystalline, consisting of three phases, namely elemental Fe, Fe_2B and FeB (JCPDS data cards nos. 87-0721, 75-1062, 76-0092). The phase FeB was present in traces, whereas phases Fe and Fe_2B were dominant. Diffraction lines of the elemental Fe were rather broad, indicating small crystallite size (below 10 nm). At 45° 2θ there was an overlap of two diffraction lines, 110 of Fe (2θ = 44.7°) and 211 of Fe_2B (2θ = 45.1°). The former line (the base of the common maximum) was broader than the latter (the upper part of the common maximum). Taking also into account the width of the Fe 200 diffraction line at 65.0° 2θ, one could conclude that the Fe_2B crystallites were bigger than the ones of Fe. The presence of α-Fe in SiO_2 coated Fe_2B particles was also detected in Ref. 10.

According to XRD results our coated particles are fully amorphous whereas those in Ref. 10 (having thiner SiO_2 shell) showed the presence of nanosize crystalline domains possibly coexisting with the amorphous phase (which showed up in Mössbauer spectra). The structure of our uncoated Fe_2B particles is probably similar to that of coated particles in Ref. 10 . This emphasizes the effect of silica coating on the atomic scale structure/amorphicity of Fe_2B-like nanoparticles which seems similar to that of silicon in Fe-B-Si type of metallic glasses.* Besides more pronounced amorphicity of SiO_2 coated particles, it is expected that oxidation is significantly reduced in comparison with uncoated particles, as was the case in Ni nanoparticles embedded into SiO_2.[11]

Typical scanning electron microscope (SEM) images for all three samples are presented in Figures 2, 3 and 4. For uncoated particles the grouping is chain-like, which is characteristic for magnetically interacting particles. However, the coated particles are grouped on piles or stacks, indicating possibly weak non-directional surface interactions.

*We thank the referee for pointing to us this analogy.

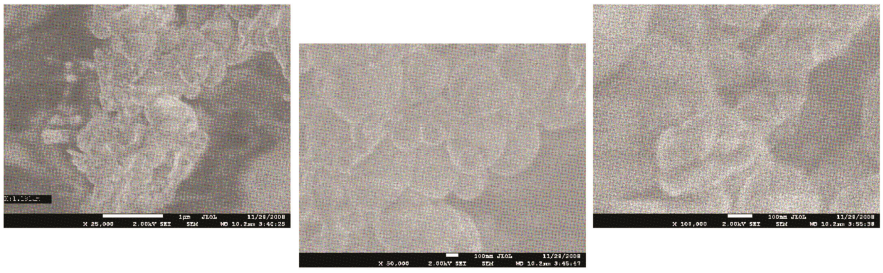

Figure 3. SEM images of Fe_2B/SiO_2 particles.

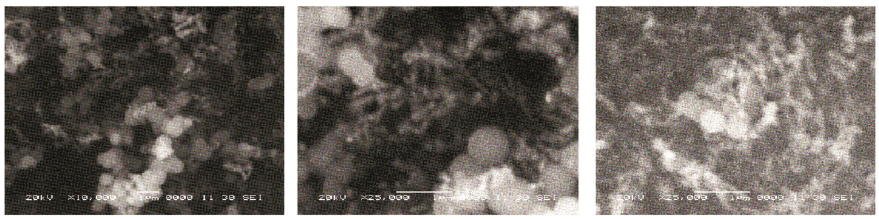

Figure 4. SEM images of $Fe_xCo_{2-x}B/SiO_2$.

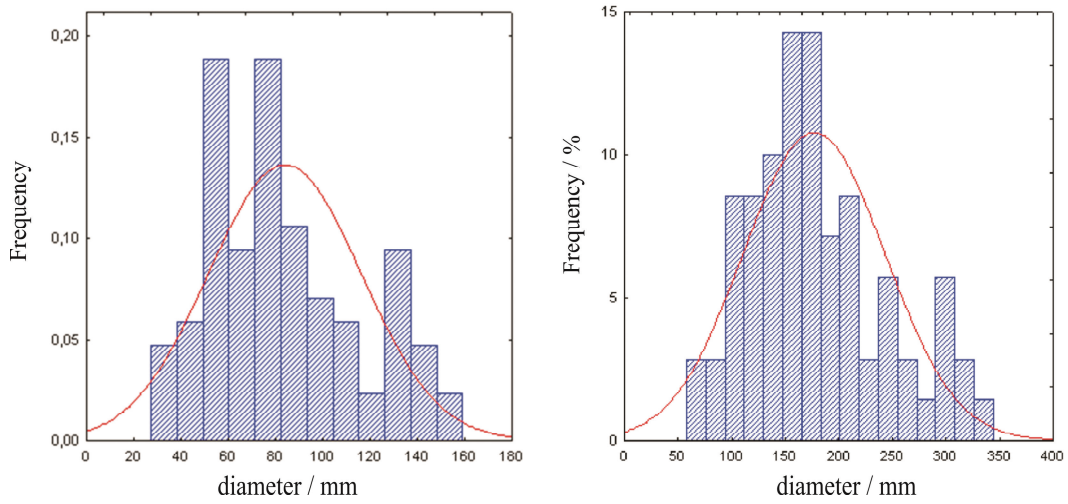

Figure 5. Size distribution of Fe_2B (left) and Fe_2B/SiO_2 (right) particles.

The statistical processing is performed measuring the grain sizes, putting the sizes into categories and fitting this by normal distribution functions. The histograms of particle sizes and the corresponding fits for uncoated and SiO_2 coated Fe_2B particles are shown in Figure 5. The distributions for both types of particles are quite broad, with a mean particle diameters about 84 nm and 177 nm for uncoated and coated particles, respectively. The distribution of particles in $FeCoB/SiO_2$ powder was similar to that for Fe_2B/SiO_2 (Figure 5) but in this case also some particles with diameters bigger than 400 nm were detected (Figure 4).

3.2 Magnetic characterization

Temperature dependence of magnetization for all samples measured upon warming the sample up in magnetic field of 0.01 T after cooling in zero field (ZFC) and after cooling in field (FC) is shown in Figure 6. The splitting between ZFC and FC curves is a sign of magnetic moment blocking in a system. The measured ZFC curves are very broad and have not the characteristic shape with single localized maximum that would point to the isolated or weakly interacting particles of narrow size distribution.[12] Instead, their outstretched shapes point to the broad distribution of characteristic sizes of particles, and in addition they could be aggregated and mutually interacting.[13,14] Also, in this broad size distribution it is possible to have a ferromagnetic component associated with bigger particles, mixed into the superparamagnetic behaviour of smaller particles. Therefore, it is somewhat ambiguous to analyse these curves quantitatively.

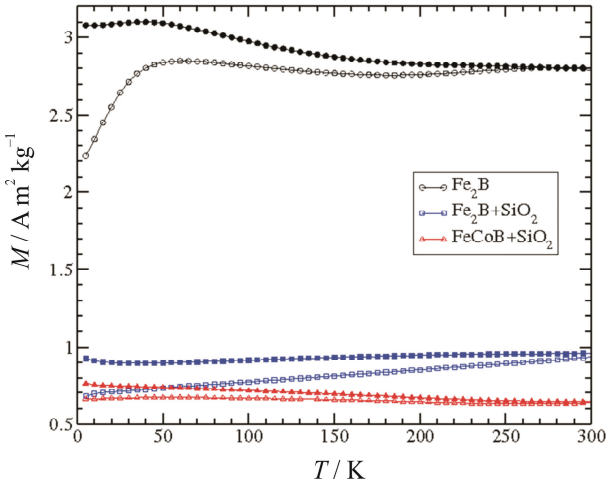

Figure 6. ZFC (open symbols) and FC (solid symbols) magnetization curves measured in magnetic field of 0.01 T.

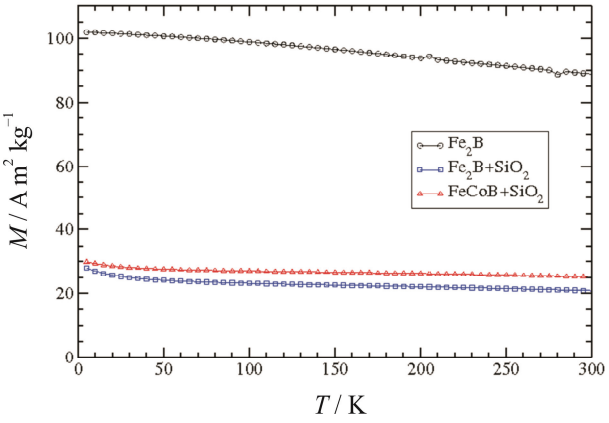

Figure 7. Temperature dependence of magnetization in field of 5 T.

Nevertheless, we could estimate the characteristic energy barrier heights U which are blocking the particles magnetization against the reorientation. The fluctuation time τ of superparamagnetic nanoparticle magnetization is given by the Neel and Brown expression $\tau = \tau_0 \exp(U/k_BT)$, where $\tau_0 = 10^{-11}$–10^{-9} s.[15] When $\tau \leq \tau_{exp}$, where τ_{exp} is time of measurement of single data point (about 30 s with MPMS5), ZFC and FC curves should overlap. For temperatures lower than the so called blocking temperature T_B the opposite ($\tau > \tau_{exp}$) applies and there is splitting between ZFC and FC curves because the system has no enough time to reach equilibrium state within time window of single point measurement. Therefore, the relation $U \approx 25k_BT$ could be used[12,15,16] to determine barrier height for uniform particles. However, for samples consisting of nanoparticles with a broad size distribution this procedure can still give at least an effective barrier height. The maxima at ZFC curves represent the temperatures at which the largest number of nanoparticles is thermally unblocked. Large difference between the temperature of maximum and the splitting temperature for Fe_2B particles in Figure 6 points to a broad distribution of barrier heights. Therefore, broad maxima at ZFC curves reflect wide distribution over sizes of particles, as well as the interaction between them.[13,14,17] With the increase of measuring field we observed that T_B decreases. This behaviour is usual for superparamagnetic materials because applied magnetic field lowers the anisotropy barriers.[16]

Taking for T_B the temperature where the splitting between ZFC and FC curves measured in relatively small applied field of 10 mT appears, that is between 260 K and 300 K for our samples, the effective barrier heights U_{eff} from 6500 to 7500 K follow. This estimated value is near to the values of energy barriers for much smaller nanoparticles of crystalline ferrites.[12,17,18] Since our smallest particles (exhibiting superparamagnetic behaviour) were still larger than those of ferrites[12] this indicates that the anisotropy energy density in our nanoparticles is much lower than in ferrites. Besides probably lower anisotropy of our material alone, this may be due to the presence of amorphicity in the prepared particles. It is generally known that the amorphous materials have much smaller magnetic anisotropy than crystalline magnets.[19] However, the estimated U_{eff} values can not be used for reliable calculation of anisotropy energies of our particles, due to unknown contribution of ferromagnetic component and of the size of particles exhibting superparamagnetic behaviour.

The high-field magnetization of coated particles show an upturn at the lowest temperatures which is absent in uncoated particles (Figure 7). This upturn of M at low temperatures points to the presence of paramagnetic component in the system of coated particles. Similar upturn was observed for $CoFe_2O_4$ nanoparticles embedded in potassium silicate.[20] At low fields (0.01 T) this upturn is less pronounced, because of prevailing nonlinear response of the superparamagnetic component. The origin of this upturn is unclear to us at present.

Magnetic hysteresis loops for the three samples are presented in Figure 8. High field magnetization behaviour shows that the saturation is still not reached and we used the magnetization at 5 T as useful for comparison with other published data. Curved shape of the hysteresis loops also points to the blocked superparamagnetic ensemble of particles, similar to the one reported for $CuFe_2O_4$ nanoparticles[12] and Al-doped Ni-ferrite.[5] This shape deviates from hysteresis of magnetically long range ordered materials (see Ref. 21 and other textbooks), particularly when high field region is considered, where the absence of saturation is connected with superparamagnetic particles.

The values of hysteresis parameters, including coercive field H_c, remanent magnetization M_r and magnetization at field of 5 T M_{5T} of our samples are pre-

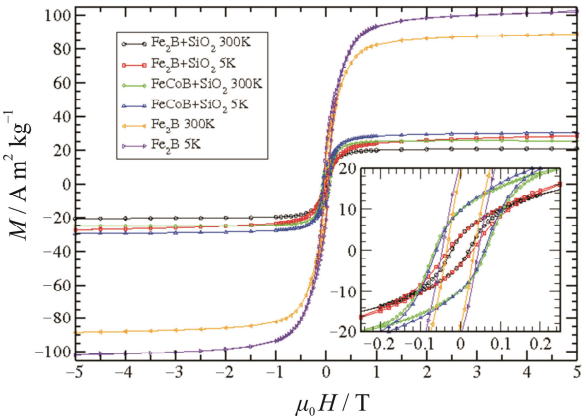

Figure 8. Magnetic hysteresis loops for all three samples at temperatures 300 and 5 K. The inset shows zoomed low-field region.

sented in Table 1. Coercive fields are bigger at 5 K than at 290 K, which is characteristic of nanoparticulated magnetic materials. Also, the observed decrease of M_{5T} from 5 to 300 K is in accordance with behaviour of magnetization for magnetic nanoparticles.[12] However, the admixture of ferromagnetic component in the samples makes the quantitative analysis of these data quite ambiguous.

Magnetic properties of the samples from different syntheses were reproducible. Slight change of the T_B and the widths of maxima were the consequences of slightly different distributions of particle sizes. Some problems with agglomeration of particles appeared when the reacted solution was left for a longer time. Also, the hydrate iron oxide formation appeared as a consequence of the too long reaction time and oxidation. The other undesired product was the precipitated SiO_2 in form of ellipsoidal blocks comparable to the size of particles. This phase reflected in magnetic properties as the decrease of mass magnetization, as well as was the case when the shells of SiO_2 around magnetic particles were too thick. To avoid these adversities the TEOS quantity should stay around the values reported in experimental section.

As mentioned in Chapter 3.1, Fe_2B nanoparticles coated with thin SiO_2 layer (≈4 nm) and with similar mean size were synthesized and characterized earlier.[10] Compared to results from Ref. 10 we obtained larger coercive field $\mu_0 H_c$ (their value is 7.3 mT) and hysteresis loops more typical for superparamagnetic particles which are of size bigger than in Ref. 10. Higher coercive field could originate from bigger particles, as higher field is needed to reorient their magnetic moment over higher barrier ($U = K \cdot V$), but a difference in mean particle sizes is too small in order to account for such a large difference in H_cs. Nevertheless, this may be consistent with broad particle size distribution of our samples, where the coercive field is determined mainly by bigger particles. Here, the possible ferromagnetic component associated with our bigger particles makes additional problem in a more quantitative analysis. Lower H_c of our SiO_2 coated Fe_2B particles compared to bare Fe_2B particles (Table 1) is consistent with observed higher amorphicity of coated particles and smaller magnetic cores of the particles. We note that nanoparticles with large H_c and large M_s (hence large hysteresis loss) are required for hyperthermia applications.

More striking is the high saturation magnetization M_s in our samples. For uncoated Fe_2B particles M_{5T} = 102 Am^2 kg^{-1} at 5 K (Table 1), which is unexpectedly high (2.23 Bohr magnetons per formula unit). It is known that nanocrystalline Fe_2B should have M_s of 80 A m^2 kg^{-1} at low temperature.[22] Higher M_s in our Fe_2B sample is probably due to the presence of iron nanoparticles, whose saturation magnetization in nanocrystalline phase is known to be 210 A m^2 kg^{-1} (Ref. 23). It follows from these values that the mass content of Fe_2B and Fe particles is 83 % and 17 %, respectively, under an assumption that these two components are the only magnetic components and that mass of other components is negligible. The presence of tiny Fe particles with size of the order of ≈10 nm or less in our powder was detected in XRD patterns (Figure 1). As mentioned earlier, Fe_2B powder from Ref. 10 also contained Fe nanoparticles in addition to about 81 % Fe_2B phase.

For our coated particles the lower saturation magnetization than in Ref. 10 (56.6 A m^2 kg^{-1} at room temperature and 1 T) reflects thicker SiO_2 shell in our sample. From the ratio of magnetization at 5 T (Figure 7) for uncoated and coated Fe_2B powder (Figures 7 and 8) we deduce the mass ratio between SiO_2 and Fe_2B ≈□3. Combining this ratio with mass densities of SiO_2 and

Table 1. Magnetic hysteresis parameters (coercive field H_c, remanent magnetization M_r and magnetization at 5 T M_{5T}) and anisotropy energy density K

Sample	$\mu_0 H_c$ / mT		M_r / A m^2 kg^{-1}		M_{5T} / A m^2 kg^{-1}		K / J m^{-3}
	300 K	5 K	300 K	5 K	300 K	5 K	
Fe_2B	34	45	18.4	21.2	88.7	103	$2.8 \cdot 10^4$
Fe_2B/SiO_2	22	31	3.32	3.48	20.8	28	$1.9 \cdot 10^4$
$FeCoB/SiO_2$	64	60	9.7	9.67	25.2	29.8	$1.6 \cdot 10^4$

Fe_2B we estimate that the thickness of coating is roughly the same as the radius of Fe_2B core. This estimate agrees very well with SEM results which find that a mean size of coated Fe_2B particles is around twice that of uncoated (Figures 2 and 3). Moreover, coercive field of our coated particles is somewhat lower than for bulk crystalline Fe_2B, that amounts 39 mT (Ref. 10). In our case, H_c is not only determined by appropriate anisotropy density and volume of particles (where the negligible interaction between separated particles is important), but also with ferromagnetic behaviour of bigger, amorphous particles.

Assuming that our particles are single domain, the Stoner-Wohlfarth model[15,24] enables to calculate the anisotropy energy density $K = MH/2h$ from hysteresis loops, where for M is used M_{5T} at 5 K that is close to the saturation magnetization. According to their calculations $h = 0.5$ should be used for samples of randomly oriented magnetic spheroids if $H = H_c$ is taken. The values for K obtained in this way are presented in Table 1. Somewhat lower values for K than in case of usual crystalline particles[17] are in accordance with the fact that the anisotropy of amorphous particles originates mainly from the shape and surface anisotropy.[25] Indeed, K for partially crystalline uncoated Fe_2B particles is larger than that for fully amorphous coated particles. These low values of K are also consistent with low estimated values for U_{eff}. A more quantitative analysis along these lines is not possible due to complex interplay of ferromagnetic and superparamagnetic behaviour.

CONCLUSION

In the reported research we achieved several goals important for both understanding and applications of ferromagnetic iron boride type nanoparticles. First, we showed that the composition of magnetic particles with amorphous structure (thus also their properties) can be selected by choosing precursors and synthesis conditions in the reaction of reduction of metal ions by use of KBH_4 or $NaBH_4$. Second, we coated the precipitated particles with silicon dioxide in order to further change the properties and stability of magnetic particles. Third, we found that sufficient quantities of nanoparticles (*e.g.* 5 g) can be produced by this method (in a short time) for the use in practical applications (for example, doping of superconductors).

Novel route of nanoparticle synthesis showed to be very efficient in producing amorphous Fe_2B core encased in SiO_2 shell. The agglomeration of uncoated particles appears to be characteristic for magnetic particle systems governed by their magnetic interactions, whereas coated particles seem to cluster as a consequence of undirected and weak interactions which make it easier to prevent their agglomeration.

Very good consistency between the results of structural (XRD, SEM) and magnetic studies was found. The observed shapes of magnetic hysteresis are reminiscent of magnetic nanoparticle systems and differ from those of bulk ferromagnets. At the same time these magnetic hystereses and low field ZFC magnetizations also deviate from those for non-interacting small magnetic particles with narrow size distribution and are best described with the interplay of ferromagnetic and superparamagnetic behaviour. This complex magnetic behaviour is probably due to very broad size distribution of our particles, with smaller particles contributing superparamagnetic behaviour and the bigger ones being ferromagnetic. The pronounced increase of coercive field with decreasing temperature is consistent with the contribution of thermally activated magnetization behaviour. In case of uncoated Fe_2B samples, at least two components seem to contribute to the magnetization, one of them having smaller blocking temperature than the other. This is in accordance with structural investigation, where the existence of two different groups of particles was observed. For coated particles, very broad rise of ZFC magnetization curve may be associated with amorphous nature of magnetic cores and/or broad distribution of magnetic particle sizes, possibly interacting. The amorphous structure of coated particles also showed up in their quite low anisotropy energy K. Properties of our particles compare favourably with those of recently reported silica coated Fe_2B particles with similar size. Our particles are fully amorphous and posses larger magnetizations and coercive fields than those from Ref. 10. Future synthesis is hoped to produce somewhat smaller particles in order to exhibit pure superparamagnetic behaviour of obtained compounds and to avoid the uncertainties in analysis caused by ferromagnetism of large particles.

Altogether, magneto-structural characteristics of obtained magnetic nanoparticles show that our samples could serve as a prosperous material for doping of superconductors, provided that smaller average particle size and narrower size distribution is achieved. Further investigation will be directed toward successful anti-agglomeration measures, too. This important item connected with their magnetic properties becomes yet crucial in mixing and dispersing the particles within superconductor.[26]

Acknowledgements. This work is supported by Unity Through Knowledge Fund (Croatia) under project UKF 1B 01/07 (webpages of the project http://www.phy.hr/~mgb2).

REFERENCES

1. R. H. Kodama, *J. Magn. Magn. Mater.* **200** (1999) 359–372.
2. J. Tejada, R. F. Ziolo, and X.X. Zhang, *Chem. Mater.* **8** (1996) 1784–1792.

3. A. Moser, K. Takano, D. T. Margulies, M. Albrecht, Y. Sonobe, Y. Ikeda, S. Sun, and E. E. Fullerton, *J. Phys. D: Appl. Phys.* **35** (2002) R157–R167.
4. Q. A. Pankhurst, J. Connolly , S. K. Jones, and J. Dobson, *J. Phys. D: Appl. Phys.* **36** (2003) R167–R181.
5. A. T. Raghavender, D. Pajić, K. Zadro, T. Mileković, P. V. Rao, K. M. Jadhav, and D. Ravinder, *J. Magn. Magn. Mater.* **316** (2007) 1–7.
6. P. Tartaj, M. P. Morales, S. Veintemillas-Verdaguer, T. González-Carreño, and C. J. Serna, *J. Phys. D: Appl. Phys.* **36** (2003) R182–R197.
7. B. Qu, X. D. Sun, J.-G. Li, Z. M. Xiu, S. H. Liu, and C. P. Xue, *Supercond. Sci. Technol.* **22** (2009) 015027 (4pp).
8. S. Wells, S. W. Charles, S. Mørup, S. Linderoth, J. van Wonterghem, J. Larsen, and M.B. Madsen, *J. Phys.: Condens. Matter* **1** (1989) 8199–8208.
9. J. Jiang, I. Dézsi, U. Gonser, and X. Lin, *J. Non-Crystalline Solid.* **124** (1990) 139–144.
10. C. Saiyasombat, N. Petchsang, I. M. Tang, and J. H. Hodak, *Nanotechnology* **19** (2008) 085705 (7pp).
11. F. C. Fonseca, G. F. Goya, R. F. Jardim, R. Muccillo, N. L. V. Carreño, E. Longo, and E. R. Leite, *Phys. Rev. B* **66** (2002) 104406-1-5.
12. D. Pajić, K. Zadro, R. E. Vanderberghe, and I. Nedkov, *J. Magn. Magn. Mater.* **281** (2004) 353–363.
13. P. Allia, M. Coisson, P. Tiberto, F. Vinai, M. Knobel, M. A. Novak, and W.C. Nunes, *Phys. Rev. B* **64** (2001) 144420 (12pp).
14. M. Knobel, W. C. Nunes, A. L. Brandl, J. M. Vargas, L. M. Socolovsky, and D. Zanchet, *Physica B* **354** (2004) 80–87.
15. S. Blundell, *Magnetism in Condensed Matter*, Oxford University Press, New York, 2001.
16. C. P. Bean and J. D. Livingston, *J. Appl. Phys.* **30** (1959) S120−129.
17. E. M. Chudnovsky and J. Tejada, *Macroscopic Quantum Tunneling of the Magnetic Moment*, Cambridge University Press, Cambridge, U.K., 1998.
18. N. Novosel, D. Pajić, A. T. Raghavender, K. Zadro, and K.M. Jadhav, *J. Phys. Conf. Ser.* **200** (2010) 072070 1–4.
19. H. Kronmüller and N. Moser, in *Amorphous Metallic Alloys*, edited by F. E. Luborsky (Butterworths, London, 1983), p. 358.
20. X. X. Zhang, J. M. Hernandez, and J. Tejada, *Phys. Rev. B* **54** (1996) 4101–4106.
21. J. Crangle, *Solid State Magnetism*, Van Nostrand Reinhold, New York, 1991.
22. E. Dorolti, P. Vlaic, E. Burzo, and C. Djéga-Mariadassou, *AIP Conf. Proc.* **899** (2007) 777–778.
23. G. F. Korznikova, A. V. Korznikov, L. A. Syutina, and Kh.Ya. Mulyukov, *J. Magn. Magn. Mater.* **196–197** (1999) 207–208.
24. E. C. Stoner and E. P. Wohlfarth, *Phil. Trans. Roy. Soc. London* **A240** (1948) 599–642, reprinted in *IEEE Trans. on Magnetics* **27** (1991) 3475–3518.
25. M. Tortarolo, R. D. Zysler, H. Troiani, and H. Romero, *Physica B* **354** (2004) 117–120.
26. N. Novosel, D. Pajić, M. Mustapić, E. Babić, A. Shcherbakov, J. Horvat, Ž. Skoko, and K. Zadro, *J. Phys. Conf. Ser.* **234** (2010) 022027.

SAŽETAK

Sinteza, strukturna karakterizacija i magnetska svojstva nanočestica željezovog borida oklopljenih ili neoklopljenih sa silicijevim dioksidom

Mislav Mustapić,[a] Damir Pajić,[a] Nikolina Novosel,[a] Emil Babić,[a] Krešo Zadro,[a] Marina Cindrić,[b] Joseph Horvat,[c] Željko Skoko,[a] Mirjana Bijelić[a] i Andrey Shcherbakov[c]

Fizički odsjek, Prirodoslovno-matematički fakultet, Sveučilište u Zagrebu, Bijenička cesta 32, HR-10000 Zagreb, Hrvatska
[b]*Kemijski odsjek, Prirodoslovno-matematički fakultet, Sveučilište u Zagrebu, Horvatovac 102a, HR-10000 Zagreb, Hrvatska*
[c]*Institute for Superconducting and Electronic Materials, University of Wollongong, Northfields Avenue, NSW 2522 Wollongong, Australia*

Nanočestice željezo borida (Fe_2B, Fe_2B oklopljene s SiO_2, $Fe_xCo_{2-x}B$ oklopljene s SiO_2) sintetizirane su redukcijom metalnih iona natrij borhidridom. Rentgenskom difrakcijom utvrđena je amorfna struktura oklopljenih nanočestica, a pretražnom elektronskom mikroskopijom utvrđena je nanočestična struktura dobivenih spojeva. Razdvajanje krivulja magnetizacije u ovisnosti o temperaturi uzorka hlađenog u odsustvu polja i u polju ukazuje na ukočenost magnetizacije superparamagnetskih nanočestica. Petlje magnetske histereze također su načelno konzistentne s ponašanjem ukočenih superparamagnetskih čestica, ali ukazuju i na postojanje višedomenskih feromagnetskih čestica. Međutim, opaženo složeno magnetsko ponašanje u skladu je sa istraživanjima strukture u kojima su pronađene dodatne faze i široka raspodjela veličina čestica.